Environ Earth Sci (2010) 60:1291–1301
DOI 10.1007/s12665-009-0269-0

ORIGINAL ARTICLE

Mangrove forest sedimentation and its reference to sea level rise, Cananeia, Brazil

Christian J. Sanders · Joseph M. Smoak · A. Sathy Naidu · Denise R. Araripe · Lucian M. Sanders · Sambasiva R. Patchineelam

Received: 18 March 2009 / Accepted: 29 July 2009 / Published online: 19 August 2009

Abstract The stability of a mangrove ecosystem in Cananeia, Brazil, is assessed based on investigations of the site-specific temporal rise in relative sea level during the past 50 years, 100-year sediment accumulation rates (SAR) and sources of organic matter (OM). Addressing this, three sediment cores were collected in a transect, intertidal mud flat, mangrove margin and well into the forest. The net SAR, as estimated by the age–depth relationships of ^{210}Pb and ^{137}Cs, is between 2.5 and 3.9 mm year^{-1}. These rates are comparable to the estimates based on the Pb and Zn contaminant markers corresponding to mining initiation in the region in 1918. Further, the SARs are lower than the rate of regional relative sea level rise (4 mm year^{-1}) as indicated by the past 50-year tide gauge record, but the rate is higher than the eustatic sea level rise (1.7 ± 0.3 mm year^{-1}). The stratigraphies of TOC/TN, $\delta^{13}C_{(OC)}$, OP and $\delta^{15}N$ indicate site-specific mangal vegetal litter, which is the predominant source of OM at all core sites, during the past century and reflects a stable mangal system over that time span.

C. J. Sanders (✉) · S. R. Patchineelam
Departamento de Geoquímica, Universidade Federal de Fluminense (UFF), Niterói, RJ, Brazil
e-mail: zinosanders@yahoo.com

J. M. Smoak · L. M. Sanders
Environmental Science, University of South Florida (USF), St. Petersburg, FL, USA

A. S. Naidu
Institute of Marine Science, University of Alaska Fairbanks (UAF), Fairbanks, AK, USA

D. R. Araripe
Departamento de Química Analítica, Universidade Federal de Fluminense (UFF), Niterói, RJ, Brazil

Keywords ^{210}Pb · ^{137}Cs · Trace metal contamination · TOC · TN · OP · $\delta^{13}C_{(OC)}$ · $\delta^{15}N$

Introduction

The relation between global warming and sea level rise (SLR) is an important issue worldwide (Hansen et al. 2005; Meehl et al. 2005). The Intergovernmental Panel on Climate Change (IPCC 2007) has projected that the rate of global sea level rise (GSLR), consequent to global warming, will be 1.8–5.9 mm year^{-1} by 2100. However, the IPCC projection refers to mean GSLR and does not apply to local or regional sea level changes.

Along the 7,500 km coast of Brazil, little is known about the relative sea level rates (RSL) or how a SLR might affect its coastal region. This is because, unlike many countries in the northern hemisphere, tide gauges have not been utilized consistently in South America. Tide gauge records are useful because they have provided trends in local sea level changes, particularly during the past century (Blasco et al. 1996). As large variations in RSL rates are found along the coastal regions of the world (Pikey and Cooper 2004), examining local sea level oscillations over the past century and comparing them to the eustatic rates provide data to develop predictive model(s) for site-specific sea level changes over the next century, in the context of global warming.

Mangrove forests tend to be most diverse and extensive on tropical sea coasts where there is a net deposition of sediments and a stable tectonic environment, among other conditions (Edwards 1995). The mangrove habituated shorelines have the potential to reveal centuries of historical sea level variations (Woodroffe et al. 1985). Studies of coastal peat cores indicate that mangrove systems have the

ability to keep pace with moderate SLR (Ellison and Stoddart 1991; Lynch et al. 1989; McKee et al. 2007; Nyman et al. 2006). Published work has shown that migration and/or mortality of the mangrove halophyte ecosystems can be caused by alterations in the sea level relative to the local sediment accumulation rates (SAR) (Blasco et al. 1996; Gilman et al. 2006; Woodroffe et al. 1985). Therefore, acquiring insights into the depositional and tectonic regimes in conjunction with the local SLR has practical use in elucidating the historical condition of a mangal system and predict its stability.

This paper examines the stability of a mangrove ecosystem located in Cananeia, SE Brazil, in the context of the predicted rise in sea level caused by global warming (IPCC 2007). Addressing this, the SAR and temporal variations in the sources of organic matter as well as organic carbon and organic phosphorus ratios (TOC/OP) were determined. This work demonstrates that the mangrove has remained the predominant source of OM during the past century [based on stratigraphies of carbon and nitrogen isotopes ($\delta^{13}C$ and $\delta^{15}N$) and organic carbon to total nitrogen ratios (TOC/TN)], reflecting the stability of the mangal ecosystem. However, considering the lower SAR relative to the regional RSL rise suggests that the system is prone to being destabilized.

Study area

The mangrove habitat under study is located along the coast of the Cardoso Island State Park (25°18.40′S and 48°23.70′W; Fig. 1). This 150 km^2 mountainous island, up to 900 m in altitude, is situated in the Cananeia lagoon-estuarine system on the southeastern coast of Brazil. The tidal range within the microtidal environment is ~82 cm (Otero et al. 2006). Fresh water influx is by continental drainage of several small rivers and the Ribeira of Iguape River, which is the principal source of sediment import to the estuary (Saito et al. 2001). The Ribeira Valley is one of the most actively mined regions for Pb and Zn and for refining Pb in Brazil. The mining activities began in 1918 and ended in 1995 (Corsi and Landim 2003). The annual average temperature and precipitation of the region are ~21°C and ~2,200 mm, respectively. Since 1954 this area has had the longest continuous running tide gauge in Brazil. Even though this coastal area is generally considered tectonically stable, an episodic earthquake of 5.2 on the Richter scale was recorded ~200 miles offshore on 22 April 2008.

Materials and methods

In 2005 sediment core samples were collected at three sites along a transect that were located 10 m into the mangrove forest (C3A), mangrove fringe (C3B) and 5 m inside of the margin in a mud flat (C3C). The cores were obtained by inserting a 7-cm-diameter plastic tube into the substrate during low tide. The sediment was extruded from the tube and sectioned at 1-cm intervals from the core top to 10 cm and subsequently at 2-cm intervals until the bottom of the

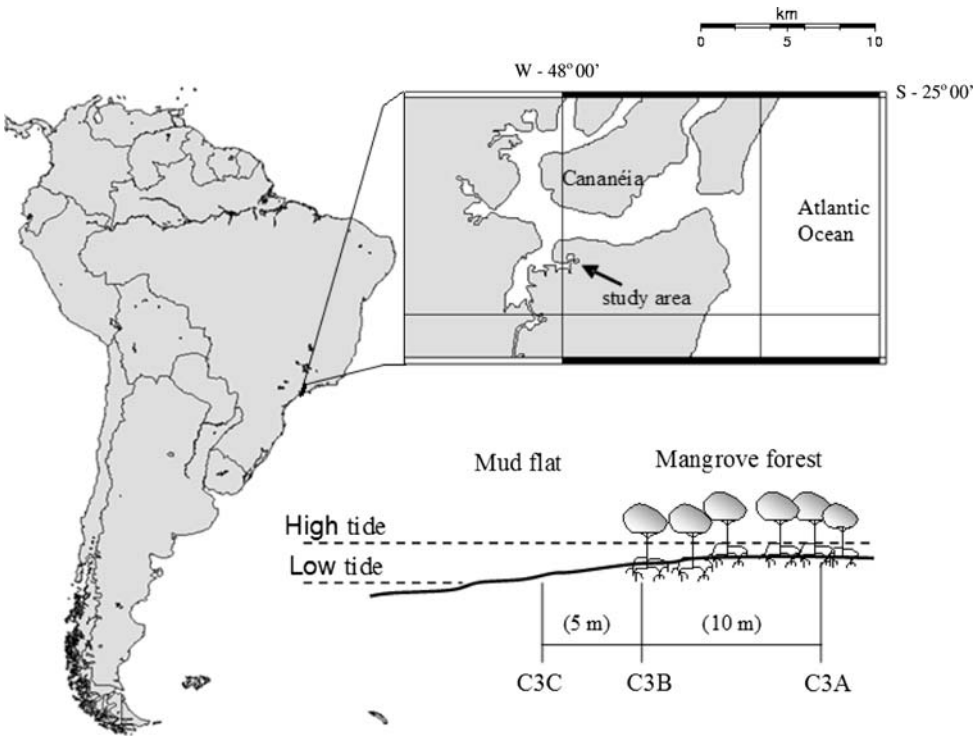

Fig. 1 Study area

core. A ~5-g split of each section was acidified to remove carbonate, dried and powdered, and a portion was taken for analyses of organic carbon (OC), total nitrogen (TN), $\delta^{13}C$ and $\delta^{15}N$ using an isotope ratio mass spectrometer (Thermo Finnigan Model Delta Plus XP), following the method outlined in Naidu et al. (2000). Organic matter (OM) was calculated by OC × 1.8 (Trask 1938). From the original wet section, a split was taken for determining dry bulk density following Baskaran and Naidu (1995). Granulometric analyses of the sections were done by a CILAS 1064 diffraction laser unit.

Total phosphorus (TP) and inorganic phosphorus (IP) were extracted from separate 0.4 g of dry pulverized sediment. The analytical procedures for determination of TP and IP were according to Grasshoff et al. (1983) using a HITACHI model U-1100 spectrometer. The organic phosphorus was derived by subtracting the inorganic phosphorus from the total phosphorus. The analytical precision was within 2% for IP and OP. The accuracies of the analyses, which were tested through certified sediment "NIST" (Nacional Institute of Standards and Technology, Estuarine Sediment-1646a), were within 0.0027 ± 0.001%, with an average of 0.0027 ± 0.002%, varying by 6%. Pearson correlation analyses were done with STATISTICA software for Windows, Release 5.1, to verify covariances among TP, IP and OP.

Sediment accumulation rates for the three cores were determined by the depth–age relationship of ^{210}Pb and ^{137}Cs. For the radionuclide analyses splits of the remaining core sections were sealed in 70-ml petri dishes for at least 3 weeks to establish secular equilibrium between ^{226}Ra and ^{214}Pb. Gamma-ray measurements were conducted by using a semi-planar intrinsic germanium high-purity coaxial detector with 40% efficiency, housed in a lead shield, coupled to a multichannel analyzer. The ^{210}Pb activity was determined by the direct measurement of 46.5 keV photopeak, while ^{226}Ra activity was calculated using the proxy ^{214}Pb (351.9 keV) (Appleby et al. 1988). Activities were calculated by multiplying the counts per minute for each radionuclide minus background counts by a factor that includes the gamma-ray intensity and detector efficiency. This factor was determined from standard calibrations using an efficiency curve obtained by measuring and analyzing a certified standard cocktail of radionuclides; this standard was certified by IRD (Instituto de Radioproteção e Dosimetria), certified no. C/87/A00. The excess ^{210}Pb ($^{210}Pb_{(ex)}$) activity was estimated by subtracting the ^{226}Ra from the total ^{210}Pb activity. Samples were counted for 86,000 s in identical geometrical cylinders. Self-absorption corrections were calculated following (Cutshall et al. 1982). The sedimentation rate was obtained through the constant initial concentration (CIC) approach outlined in (Appleby and Oldfield 1992). Sample depth intervals were normalized for sediment mean fine grain. Cesium-137 activities were determined from the 663.7 keV gamma peak.

The ^{210}Pb and ^{137}Cs-based geochronologies of the cores were supplemented by those based on ages inferred from the contaminant history of Pb and Zn in the study region. It is assumed that the first significant increase in Pb and Zn in the three cores resulted from anthropogenic input consequent to the initiation of mining of the two metals in 1918. In this context, the stratigraphic variations in Pb and Zn were determined in the three cores. To this end, a ~2-g split of each of the core sections was analyzed for Zn and Pb. The values of the two metals were normalized against Al concentrations in core sections to account for granulometric differences in the metal chemistry (Mason et al. 2004). The Al-normalized Pb and Zn values were then plotted against the core depths for the three individual cores.

The three elements (Al, Pb and Zn) were analyzed through optical emission spectrometry inductively coupled plasma, using a Joby-Yvon ULTIMA II spectrometer. Sediment solutions were obtained by digestion with a mixture of nitric acid and hydrochloric acid (4:1), in a microwave (model MULTIWAVE of Anton Paar), and the resulting solutions were filtered with acid-rinsed 0.45 μm membrane. All the material used was pre-cleaned in 10% HCl and washed with demineralized water. Measurement errors were within 10%.

Results and discussion

Two aspects of the investigation in this work were addressed: first, on the stability of the mangrove forest habitat using stratigraphic variations of TOC, TN, TOC/TN, TP, OP, $\delta^{13}C_{(OC)}$ and $\delta^{15}N$. Second, we examined the SAR in the context of RSL rise in the area and global SLR models.

Mangrove forest stability

The concentrations of TOC, TP and TN in sections of the three cores are provided in Table 1a–c. A net significant decreasing trend may be seen in the depth profiles of the TOC, TP and TN from the surface, probably reflecting an increasing degradation with depth in the mangrove litter (Chen and Twilley 1999; Cahoon and Lynch 1997; Kristensen et al. 2000; Lallier-Verges et al. 1998; Lynch et al. 1989). Further, a relatively greater amount of OM in a landward direction, coinciding with decreasing tidal influence, is generally noted. Obviously, this trend is related to a progressively higher depositional flux of vegetal litter corresponding to denser and more stable development of mangrove forest landward (Ferreira et al. 2007).

Table 1 Organic and metal profile of cores

Depth (cm)	TOC (%)	TN (%)	$\delta^{13}C$	$\delta^{15}N$ (0/00)	TP (μg/g)	OP (μg/g)	Pb/Al[a]	Zn/Al[a]
(a)								
0–2	6.50	0.45	−28.81	1.73	580	350	3.51	20.50
2–4	7.50	0.48	−28.63	0.50	586	269	2.70	9.69
4–6	6.27	0.39	−28.16	0.06	448	302	2.81	10.85
6–8	6.20	0.37	−28.08	0.20	856	296	3.01	16.87
8–10	5.65	0.30	−28.06	−0.14	356	203	3.51	26.19
10–14	7.07	0.34	−28.17	−0.40	352	235	4.11	37.22
14–18	4.31	0.24	−27.57	1.74	374	198	3.31	19.04
18–22	6.61	0.20	−27.42	1.16	345	203	3.08	20.36
22–26	6.02	0.28	−26.76	0.66	191	150	4.73	41.65
26–30	5.56	0.24	−26.97	1.93	426	107	3.42	21.36
30–34	4.95	0.21	−26.93	2.18	280	80	2.80	18.71
34–38	4.73	0.20	−26.80	2.00	295	96	2.35	16.32
38–42	4.24	0.18	−26.52	2.17	316	116	2.37	11.25
(b)								
0–2	6.44	0.48	−27.11	2.87	600	332	1.24	27.05
2–4	7.49	0.50	−27.70	2.71	555	328	1.23	16.61
4–6	7.05	0.47	−27.81	2.71	540	288	1.29	12.53
6–8	7.17	0.45	−27.90	3.22	513	305	1.10	15.49
8–10	5.77	0.35	−27.87	2.92	456	267	1.34	13.19
10–14	5.44	0.29	−27.66	2.99	411	227	1.64	8.31
14–18	3.39	0.17	−27.33	2.88	256	93	2.00	8.71
18–22	2.96	0.15	−26.96	3.06	296	191	2.88	12.53
22–26	4.00	0.20	−27.30	2.84	291	153	1.47	6.79
26–30	2.80	0.15	−26.78	3.30	319	101	2.38	12.38
30–34	2.92	0.16	−26.90	3.34	287	146	0.98	5.43
34–38	2.62	0.13	−26.62	3.01	292	118	2.91	13.87
38–42	1.81	0.09	−26.82	3.13	314	154	1.65	6.95
(c)								
0–2	3.53	0.25	−26.76	2.93	403	221	3.09	10.68
2–4	3.88	0.27	−27.06	2.95	396	236	2.31	8.65
4–6	3.46	0.23	−27.01	3.07	313	205	3.05	10.79
6–8	3.65	0.23	−27.24	3.03	292	162	3.12	11.17
8–10	3.60	0.22	−27.41	3.03	288	151	3.31	12.01
10–14	3.70	0.22	−26.94	3.16	300	194	3.56	12.49
14–18	3.71	0.21	−27.25	3.31	283	122	3.34	11.32
18–22	3.75	0.21	−26.97	3.22	292	164	2.28	9.32
22–26	3.52	0.20	−26.76	3.25	272	129	1.99	8.01
26–30	2.39	0.13	−27.15	2.97	248	94	3.49	12.37
30–34	1.61	0.09	−26.62	3.06	234	114	1.46	5.32
34–38	0.50	0.04	−27.07	3.96	114	16	1.54	4.59
38–42	0.48	0.04	−26.68	3.28	123	1	1.38	3.85
42–44	0.34	0.03	−26.83	4.33	85	39	1.75	4.01
44–48	0.26	0.03	−26.59	5.02	99	61	1.89	3.22

[a] Al × 1,000

It would seem that the TN enrichment in the surface layers is likely a result either from tidal fluxes in the intertidal area by marine particles rich in TN (Allison et al. 2003) and/or to higher bacterial biomass at the surface. A scavenging of TN from biological activity or an increasing mineralization of OM in the subsurface layers of the cores

Table 2 Physical characterization and $^{210}Pb_{ex}$ data of sediment cores

Depth (cm)	Dry bulk density	Clay (%)	Silt (%)	Sand (%)	Porosity (%)	$^{210}Pb_{ex}$ (Bq/kg)
(a)						
0–1	0.37	9.8	75.1	15.1	84.89	179.26 ± 18.43
1–2	0.41	9.2	69.8	21.0	83.28	156.19 ± 11.28
2–3	0.38	17.9	65.6	16.5	84.53	153.37 ± 12.32
3–4	0.37	18.1	66.4	15.5	85.13	122.09 ± 9.38
4–5	0.42	14.3	64.9	20.8	82.94	124.85 ± 10.10
5–6	0.41	14.0	63.6	22.5	83.11	137.80 ± 12.74
6–7	0.40	16.4	60.9	22.7	83.57	81.47 ± 6.16
7–8	0.46	13.5	50.4	36.1	81.28	85.62 ± 7.16
8–9	0.44	15.4	56.5	28.1	82.19	80.32 ± 6.27
9–10	0.48	14.3	52.3	33.4	80.64	43.29 ± 3.65
10–12	0.45	12.8	45.5	41.7	81.68	35.27 ± 2.65
12–14	0.48	13.9	49.3	36.8	80.51	33.86 ± 2.72
14–16	0.58	15.6	43.8	40.6	76.31	31.27 ± 2.19
16–18	0.58	16.5	46.4	37.1	76.27	27.49 ± 2.08
18–20	0.54	16.9	46.2	36.9	77.97	8.91 ± 0.80
20–22	0.52	18.5	50.6	30.9	78.81	9.75 ± 0.90
22–24	0.52	16.2	43.7	40.1	79.03	12.95 ± 1.30
24–26	0.57	13.9	37.4	48.7	76.79	8.97 ± 0.88
26–28	0.58	12.5	45.7	41.8	76.27	11.88 ± 1.49
28–30	0.64	10.3	38.0	51.7	73.93	11.63 ± 1.29
32–34	0.62	13.7	37.2	49.1	74.74	9.77 ± 1.05
34–36	0.73	14.0	38.2	47.8	70.27	8.41 ± 0.86
36–38	0.84	12.5	41.0	46.5	65.77	−1.84 ± 0.27
38–40	0.78	11.1	36.2	52.7	68.47	5.78 ± 0.85
40–42	0.64	17.3	40.4	42.3	73.83	−8.53 ± 0.25
42–44	0.64	14.0	32.6	53.5	73.87	
(b)						
0–1	0.47	17.1	60.8	22.1	81.09	294.61 ± 22.9
1–2	0.49	17.4	61.6	21.0	80.28	204.19 ± 19.66
2–3	0.43	18.7	67.3	14.0	82.40	322.23 ± 33.10
3–4	0.42	19.1	68.7	12.2	82.95	305.10 ± 32.41
4–5	0.41	17.6	65.7	16.7	83.39	311.92 ± 34.67
5–6	0.37	17.2	64.3	18.5	85.06	210.18 ± 19.47
6–7	0.39	17.7	63.5	18.8	84.23	156.90 ± 14.42
7–8	0.46	14.3	51.2	34.5	81.34	260.22 ± 25.28
8–9	0.44	17.5	43.1	39.4	82.34	232.10 ± 24.63
9–10	0.51	20.9	51.5	27.6	79.46	219.23 ± 17.58
10–12	0.58	13.9	46.2	39.9	76.53	129.50 ± 10.02
12–14	0.61	11.2	37.5	51.3	75.19	89.43 ± 7.76
14–16	0.74	13.4	39.7	46.9	70.12	52.08 ± 4.06
16–18	0.75	9.0	26.8	64.2	69.78	68.90 ± 5.91
18–20	0.75	12.2	32.6	55.2	69.33	42.24 ± 3.88
20–22	0.79	10.4	27.8	61.8	68.14	36.06 ± 3.65
22–24	0.77	14.3	45.3	40.4	68.48	58.75 ± 6.68
24–26	0.78	8.4	26.7	64.9	68.11	17.33 ± 1.79
26–28	0.77	8.3	32.3	59.4	68.51	23.80 ± 2.24
28–30	0.76	7.3	28.5	64.2	69.16	23.15 ± 2.16

Table 2 continued

Depth (cm)	Dry bulk density	Clay (%)	Silt (%)	Sand (%)	Porosity (%)	$^{210}Pb_{ex}$ (Bq/kg)
32–34	0.73	11.0	36.2	52.8	70.38	4.54 ± 0.38
34–36	0.83	9.8	32.4	57.8	66.49	13.64 ± 1.09
36–38	0.85	6.6	24.1	69.3	65.55	7.15 ± 0.70
38–40	0.70	11.7	42.9	45.4	71.49	20.98 ± 2.37
40–42	0.89	9.2	36.7	54.1	63.98	−8.53 ± 0.97
42–44	0.99	9.8	39.1	51.1	59.96	
(c)						
0–1	0.68	7.5	66.0	26.5	72.67	104.52 ± 4.47
1–2	0.66	7.0	62.0	31.0	73.08	93.49 ± 5.71
2–3	0.66	8.8	62.3	28.9	73.39	94.13 ± 6.23
3–4	0.63	9.0	63.6	27.4	74.49	94.54 ± 4.73
4–5	0.61	12.5	59.1	28.4	75.12	94.74 ± 4.73
5–6	0.69	13.0	61.8	25.2	71.85	100.53 ± 4.91
6–7	0.64	7.9	63.5	28.6	74.09	104.50 ± 4.66
7–8	0.61	7.4	60.1	32.5	75.73	98.54 ± 4.71
8–9	0.65	11.4	52.2	36.4	73.57	100.44 ± 4.82
9–10	0.68	12.1	55.4	32.5	72.58	85.48 ± 3.69
10–12	0.65	12.1	51.4	36.5	73.53	60.21 ± 2.32
12–14	0.71	10.4	44.4	45.2	71.32	59.15 ± 2.32
14–16	0.70	9.1	45.6	45.3	71.72	29.45 ± 1.24
16–18	0.69	10.1	50.6	39.3	72.16	50.11 ± 2.22
18–20	0.71	13.2	55.7	31.1	71.27	37.35 ± 1.73
20–22	0.61	12.7	53.4	33.9	75.24	28.01 ± 1.62
22–24	0.74	10.4	43.6	46.0	69.99	23.35 ± 1.29
24–26	0.82	10.0	42.0	48.0	66.94	25.10 ± 1.27
26–28	0.88	10.3	45.8	43.9	64.45	15.75 ± .092
28–30	0.94	10.1	44.8	45.1	61.96	10.15 ± 0.60
32–34	0.91	9.2	45.8	45.0	63.30	10.85 ± 0.64
34–36	1.07	9.3	46.5	44.2	56.62	11.51 ± 0.70
36–38	1.13	8.8	42.0	49.2	54.39	−0.32 ± 0.02
38–40	1.16	12.1	57.3	30.6	53.10	2.79 ± 0.11
40–42	1.19	12.7	57.3	30.0	51.81	−0.89 ± 0.05
42–44	1.22	11.9	53.3	34.8	50.40	2.54 ± 0.19
44–46	1.27	12.4	52.7	35.0	48.48	4.13 ± 0.30
46–48	1.33	12.4	52.7	35.0	46.20	−0.54 ± 0.04
48–50	1.26	11.4	45.4	43.2	49.09	0.39 ± 0.69

may explain a slight decrease in the TN concentrations down core. Other studies suggest that this profile is characteristic of a recent introduction of fresh OM from vascular plants to surface sediments (Lallier-Verges et al. 1998; Marchand et al. 2006).

Phosphorous concentrations may also provide insight into OM origins in marine sediments (Mach et al. 1987), specifically based on OC/OP ratios (Ruttenberg and Goni 1997). For instance, terrestrial plants have values between 300 and 1,300 (Ruttenberg and Goni 1997), while marine phytoplankton has an average of approximately 100 (Redfield et al. 1963). Consideration of the sediment OC/OP values (average value of 253 and ranging from 43 to 621) indicates marine input and/or a rapid immobilization of OP that may occur during OM decomposition (Tables 1, 2) (Alongi 1991; Holmboe et al. 2001).

The overall close ranges of TOC/TN and TOC/OP of the cores (Table 1) suggest a consistent depositional flux of OM perhaps derived from the same source. As mangrove ecosystems have a high capacity of retaining and recycling most nutrients within the sediment column (Kristensen et al. 2000; Twilley et al. 1986), this trend may be expected in a robust mangrove forest.

Although increased down-core degradation of OM may occur, the signature of the sources of sediment OM most likely remains preserved in sediment cores as expressed in their carbon and nitrogen isotopic composition (Meyers 1994). This is likely the case in this study area, as indicated by the $\delta^{13}C_{(OC)}$ and $\delta^{15}N$ results (Table 1a–c).

As mangrove vegetation is unique in that it survives in specific intertidal zones, specific geochemical proxies have been implied for the three core locations to better understand the characterization of the sediment being depositing in each specific region of the mangrove system. Core C3A displays general enrichment in the $\delta^{13}C_{(OC)}$ in the lower depths of the profile. This trend may be explained by relatively longer microbial respiration down the core that induces an isotope fractionation depleting mineralized CO_2 in ^{13}C and enriching residual degraded particulate OM in ^{13}C (Mariotti and Balesdent 1990; Mazuka and Shunula 2006). As core C3A is within the higher reaches of the forest and is inundated by tides for relatively shorter periods of time, this site is aerated for longer time intervals, thus increasing the oxidation of the OM being deposited at this site. Cores C3B and C3C are situated in the margin and mud flat region of the mangrove ecosystem, being inundated for longer periods of time. Because isotopic changes due to OM degradation are less significant in areas under the water surface, there is an expected smaller variation in the $\delta^{13}C_{(OC)}$ along these cores (Lallier-Verges et al. 1998; Lehmann et al. 2002).

In mangrove systems, sediments further inland typically have lower $\delta^{15}N$ values (Fry et al. 2000), as is the case for core C3A. These lower $\delta^{15}N$ values may be associated to the higher concentrations in OM, favoring a fractionization by plants that selectively choose ^{14}N, thereby increasing the ^{15}N concentrations, reflected in sediments having lower $\delta^{15}N$ values (Mazuka and Shunula 2006). Another possible factor in the higher $\delta^{15}N$ in core C3B and C3C is that they are in areas of the tidal flat being exposed to tidal inundation for longer periods of time. As oceanic nitrate has relatively higher $\delta^{15}N$, tidal inundation plays a larger role in the C3B and C3C than in the C3A $\delta^{15}N$ values, which is less significant farther inland (Table 1a–c).

The relatively low $\delta^{13}C_{(OC)}$ and $\delta^{15}N$ are typical values relating to a terrestrial OM source, likely from mangrove vegetation (Naidu et al. 2000 and references therein; Bouillon et al. 2003, 2004; Lallier-Verges et al. 1998; Mazuka and Shunula 2006; Woller et al. 2003). The consistent similar values throughout the cores in the carbon and nitrogen isotopes ($\delta^{13}C$ and $\delta^{15}N$) and TOC/N suggest that the sources of OM for the mangal forest has been invariable during the past ~100 years and that the source has been terrigenous and likely local from the mangal litter. Indeed, when the values of $\delta^{13}C_{(OC)}$ are plotted against those of TOC/TN, the scatter plots lie in a cluster that is attributed to C3 plants (Meyers 2003), particularly to mangrove vegetation (Bouillon et al. 2003; Bouillon et al. 2004; Lallier-Verges et al. 1998) (Fig. 2). The implication of the above is that the mangal forest in the study area has remained stable during the past century and that the stratigraphic variations are of a typical mangrove forest.

Sediment accumulation rates

Excess ^{210}Pb

A net down core decrease in $^{210}Pb_{(ex)}$ activities is seen in all three cores (Table 2a–c), which can be attributed to a few factors. The varying mud content (<63 μm size fraction) in the cores (Table 2a–c) could be a factor in the $^{210}Pb_{(ex)}$ distribution (Ravichandran et al. 1995). However, in this study the granulometric influence was minimized by normalizing the $^{210}Pb_{(ex)}$ activities to the mud fraction (Table 2a–c). After normalization, the log profiles of $^{210}Pb_{(ex)}$ were found to decrease linearly down the core (Fig. 3a–c), implying a consistent rate of sedimentation (Appleby and Oldfield 1992). Following this, the CIC dating method was applied to establish the geochronology of the three cores. The statistics related to the cores' $^{210}Pb_{(ex)}$ distribution are in figures and as follows: C3A ($n = 15$; $p < 0.05$) from the surface to the 19 cm mark; C3B ($n = 16$; $p < 0.05$) 6.5 to the 35 cm interval; C3C ($n = 14$; $p < 0.05$) between the 6.5 and 33 cm depth.

Apparently the upper 6.5-cm layers in cores C3B and C3C were reworked and, therefore, excluded in the above statistical analyses. In the mangrove forest core (C3A), the absence of a mixed surface layer agrees with the fact that

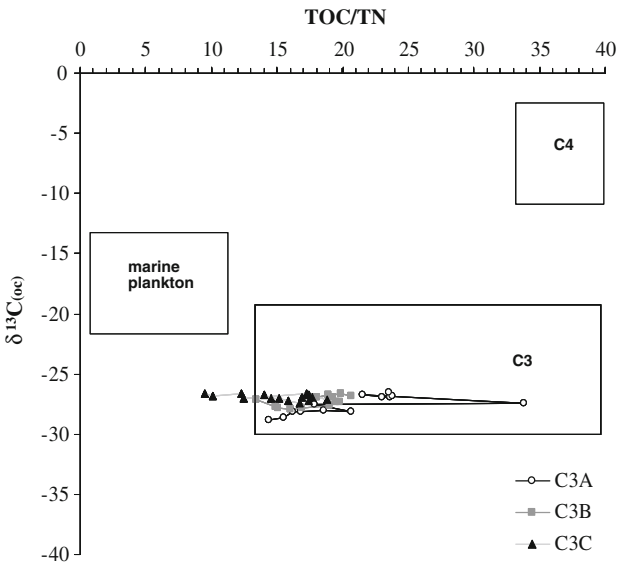

Fig. 2 TOC versus $\delta^{13}C_{(OC)}$

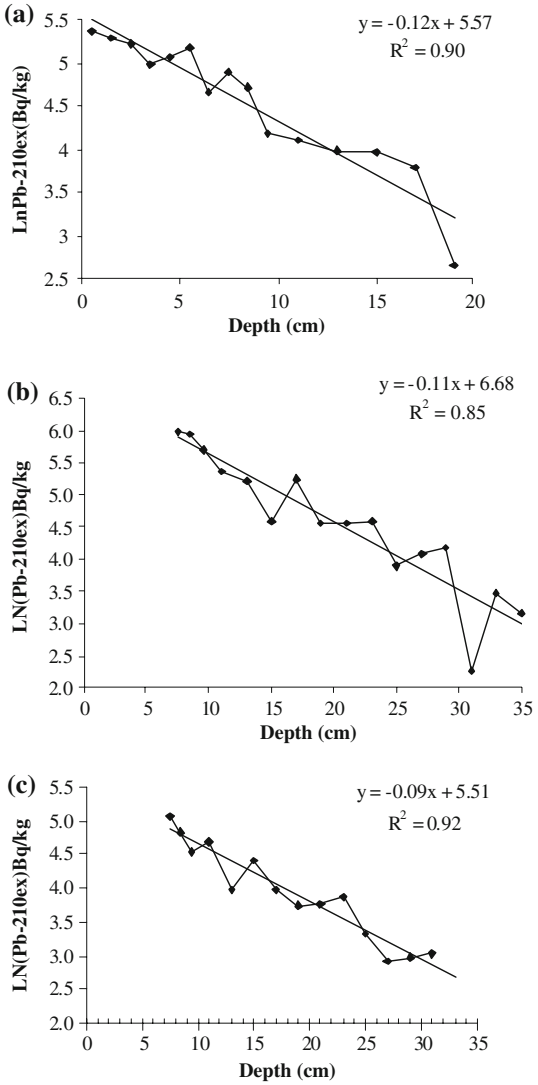

Fig. 3 Mud-normalized $^{210}Pb_{ex}$ distribution as used for SAR; **a** C3A = 2.5 mm year^{-1}, **b** C3B = 2.9 mm year^{-1}, **c** C3B = 3.9 mm year^{-1}

bioturbation and physical reworking of sediments may be negligible within salt marshes (Zwolsman et al. 1993). Along the transect, the SAR increased from 2.5 and 2.9 to 3.9 mm year^{-1}, respectively. The ^{137}Cs activities, which are often used to confirm the CIC ^{210}Pb dating model (Sanders et al. 2006), were above the detection limits in all except a few sections from specific depths of the cores. The depth where ^{137}Cs activity is highest was considered to correspond to 1963, based on which there was a SAR of 2.6 mm year^{-1} in the central forest (C3A), 3.4 mm year^{-1} in the forest margin (C3B) and 3.9 mm year^{-1} in the mud flat (C3C). Therefore, in this study the SAR estimates based on ^{137}Cs markers are in close agreement with those based on the ^{210}Pb model (Fig. 4).

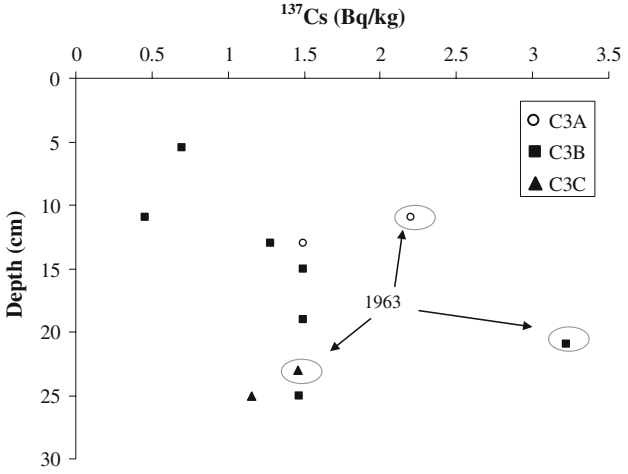

Fig. 4 Detectable ^{137}Cs activity versus depth

Trace metal signatures

Sediment accumulation rates were also estimated through evidence left by trace metal (Pb and Zn) contamination from mining activity adjacent to the study area. The Al-normalized Pb and Zn contents in the cores are listed in Table 1a–c. A sharp increase in the Pb/Al and Zn/Al ratios can be seen in the C3A core at the 24-cm mark. The C3C core shows a relatively less dramatic spike in both Pb/Al and Zn/Al ratios at the 28-cm mark. However, no clear relative Pb/Al or Zn/Al sedimentary shifts were identified in the C3B core. The spikes identified in cores C3A and C3C are assumed to coincide with Zn and Pb mining activity in 1918 (Corsi and Landim 2003). Considering the year (1918) mining activity and assuming steady sediment depositional flux since then, SAR were obtained as follows: 2.7 mm year^{-1} in the central mangrove forest (core C3A) and 2.5 mm year^{-1} in the mud flat (core C3C). These rates are comparable to those based on the ^{210}Pb and ^{137}Cs methods.

Sea level records

The Cananeia SARs are significantly lower than the local net sea level rise (SLR) as recorded by the nearby time-series tide gauge. This tide guage indicated that the sea level rose approximately 4.0 mm year^{-1} from 1954 to 2004 (Fig. 5, after the University of Hawaii http://www.soest.hawaii.edu/UHSLC/, run through the NIMED program). The SARs estimated for this study area (2.5–3.9 mm year^{-1}), used to imply RSL, are substantially higher than the rates found in mangrove forests further north (Sanders et al. 2008; Smoak and Patchineelam 1999), ~1.8 mm year^{-1}. Explanations for the discrepancies between the SAR and SLR mentioned above are:

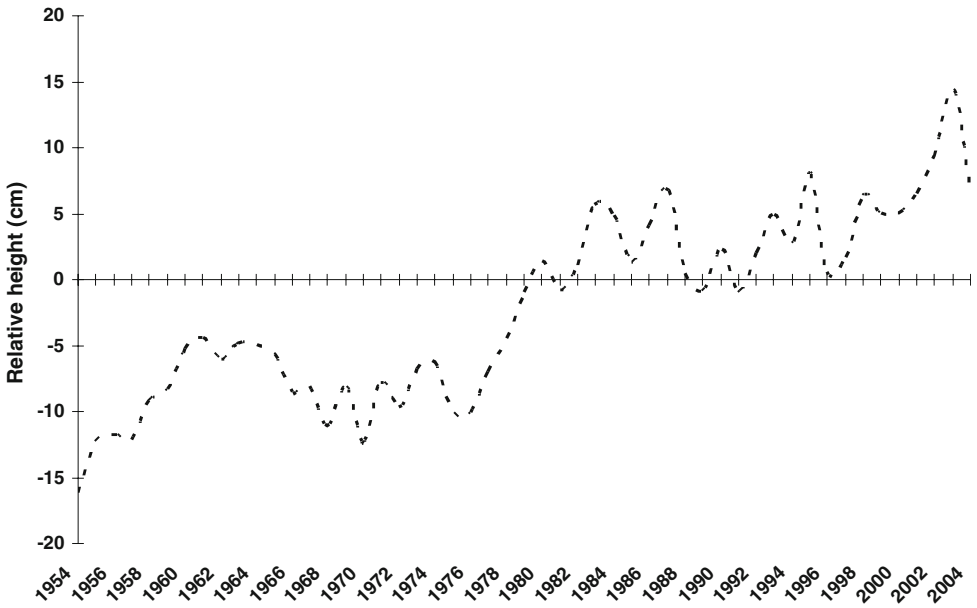

Fig. 5 Yearly tide gauge records from 1954 to 2004

1. Relative sea levels (RSL) may vary from one region to another (Harvey et al. 2002); therefore, rates indicative of a sea level rise (SLR) taken further north may not be comparable to this area. This is particularly true in Cananeia, which on 22 April 2008 was found by the USGS to be tectonically unstable, as has been noted by the recent offshore earthquake of 5.2 on the Richter scale.
2. As the Cananeia tide gauging only began 50 years ago and large decadal variation is seen in this record (Fig. 5), the duration may not be sufficient to detect an accurate sea level trend. This point is well made by Pirazzoli (1986) and is evident in this study area.
3. Given these parameters, assertions based on factors other than the eustatic sea level rise are affecting this region, and the global models may not apply for determining current and future rates in this area.

Conclusion

From the onset of this study, it was thought that the study area was tectonically stable, but could not explain the tide gauge data nor, after results were obtained, the relatively high sedimentation rates in this stable mangrove forest. That was until an earthquake was measured offshore in April 2008. The tectonic instability in the region may explain the relatively high RSL rise inferred by the tide gauge (50 years) as well as the stable SARs (over 100 years) found in the mangrove forest. As these data were not in agreement with estimates of the global mean SLR of 1.7 ± 0.3 mm year^{-1} [from 1870 to 1992 (WCRP 2006)], it is suggested that factors other than the eustatic sea level rise are affecting the sea level changes in this Brazilian region. This being so, global models to predict future rates of SLR as presented by the IPCC (2007) must be considered with some caution.

This study in the Cananeia mangrove system demonstrates that the RSL could vary from one coastal area to another. Therefore, to predict the affect of eustatic sea level rise on any given coastal region, it is critical that local, site-specific estimates of SLR must be elucidated. We also show the importance of determining the SAR on global SLR models, especially where tide gauges have not yet been installed or not been in use for a period of time sufficient to determine sea level trends.

Acknowledgments This work was funded by the Conselho Nacional de Desenvolvimento Científico e Tecnológico (CNPq), Brazil, and Fulbright support to J.M.S. We would like to acknowledge the Instituto de Radioprotecao e Dosimetria (IRD) for supplying a certified radionuclide cocktail that was used for calibrating the gamma-ray detector. The cost of the analyses of the sediment carbon and nitrogen and their isotopes were met from funds available to A.S.N. from the Institute of Marine Science, University of Alaska Fairbanks.

References

Allison MA, Khan SR, Goodbred SL Jr, Kuehl SA (2003) Stratigraphic evolution of the late Holocene Ganges–Brahmaputra lower delta plain. Sediment Geol 155:317–342

Alongi DM (1991) The role of intertidal mudbanks in the diagenesis and export of dissolved and particulate material form the fly delta, Papua New Guinea. Exp Mar Biol Ecol 149:81–107

Appleby PG, Oldfield F (1992) Application of lead-210 to sedimentation studies. In: Ivanovich M, Harmon S (eds) Uranium series

disequilibrium: application to earth, marine and environmental science. Oxford Science Publications, UK, pp 731–783

Appleby PG, Nolan PJ, Oldfield F, Richardson N, Higgitt SR (1988) Pb-210 dating of lake sediments and ombrotrophic peats by gamma assay. Sci Total Environ 68:157–177

Baskaran M, Naidu AS (1995) ^{210}Pb-derived chronology, and the fluxes of ^{210}Pb and ^{137}Cs isotopes into continental shelf sediments, East Chukchi Sea, Alaskan Arctic. Goechimica et Cosmochimica Acta 59:4435–4448

Blasco F, Saenger P, Jandoet E (1996) Mangroves as indicator of coastal change. Catena 27:167–178

Bouillon S, Dahdouh-Guebas F, Rao AVVS, Koedam N, Dehairs F (2003) Sources of organic carbon in mangrove sediments: variability and possible ecological implications. Hydrobiologia 495:33–39

Bouillon S, Moens T, Koedam N, Dahdouh-Guebas F, Baeyens W, Dehairs F (2004) Variability in the origin of carbon substrates for bacterial communities in mangrove sediments. FEMS Microbiol Ecol 49:171–179

Cahoon DR, Lynch CJ (1997) Vertical accretion and shallow subsidence in a mangrove forest of Southwestern Florida, USA. Mangroves Salt Marshes 1:173–186

Chen R, Twilley RR (1999) A simulation model of organic matter and nutrient accumulation in mangrove wetland soils. Biogeochemistry 44:93–118

Corsi AC, Landim PMB (2003) Chumbo, zinco e cobre em sedimentos de corrente nos Ribeiroes Grandes, Perau e Canoas, e Corrego Barrinha no municipio de Adrianopolis (Valle do Ribeira, PR). Geociencias 22:49–61

Cutshall NH, Larsen IL, Olsen CR (1982) Direct analysis of ^{210}Pb in sediment samples: self-absorption corrections. Nucl Instrum Methods 206:309–312

Edwards AJ (1995) Impact of climatic change on coral reefs, mangroves, and tropical seagrass ecosystems. In: Eisma D (ed) Climate change. CRC Press Inc, Boca Raton, pp 209–234

Ellison JC, Stoddart DR (1991) Mangrove ecosystem collapse during predicted sea-level rise—Holocene analogs and implications. J Coastal Res 7:151–165

Ferreria TO, Vidal-Torrado P, Otero XL, Macias F (2007) Are mangrove forests substrates sediments or soils? A case study in southeastern Brazil. Catena 70:79–91

Fry B, Berna AL, Rossb MS, Meederb JF (2000) δ^{15}N Studies of nitrogen use by the red mangrove, *Rhizophora mangle* L. in South Florida. Estuar Coast Shelf Sci 50:291–296

Gilman EL et al (2006) Adapting to Pacific Island mangrove responses to sea level rise and climate change. Climate Res 32(3):161–176

Grasshoff K, Ehrardt M, Kremling K (1983) Methods of seawater analysis. Verlag Chemie, Weinheim, p 419

Hansen J et al (2005) Earth's energy imbalance: confirmation and implication. Science 308:1431–1435

Harvey N, Belperio A, Bourman R, Mitchell W (2002) Geologic, isostatic and anthropogenic signals affecting sea level records at tide gauge sites in southern Australia. Global Planet Chang 32:1–11

Holmboe N, Kristensen E, Andersen F (2001) Anoxic decomposition in sediments from a tropical mangrove forest and the temperate Wadden Sea: implications of N and P addition experiments. Estuar Coast Shelf Sci 53:125–140

IPCC (2007) Climate change 2007: the physical science basis, intergovernmental panel on climate change. Paris

Kristensen E, Andersoen FO, Holmboe N, Holmer M, Thongtham N (2000) Carbon and nitrogen mineralization in sediments of the Bangrong mangrove area, Phuket, Thailand. Aquat Microbial Ecol 22:199–213

Lallier-Verges E, Perrussel BP, Disnar J, Baltzer F (1998) Relationships between environmental conditions and the diagenetic evolution of organic matter derived from higher plants in a modern mangrove swamp system (Guadeloupe, French West Indies). Org Geochem 29(5–7):1663–1686

Lehmann MF, Bernasconi SM, Barbier A, McKenzie JA (2002) Preservation of organic matter and alteration of its carbon and nitrogen isotope composition during simulated and in situ early sedimentary diagenesis. Geochimica et Cosmochimica Acta 66(20):3573–3584

Lynch CJ, Meriwether JR, McKee BA, Vera-Herrera F, Twilley RR (1989) Recent accretion in mangrove ecosystems based on Cs-137 and Pb-210. Estuaries 12(4):284–299

Mach DM, Ramirez A, Holland HD (1987) Organic phosphorus and carbon in marine sediments. Am J Sci 278:429–441

Marchand C, Lallier-Verge's E, Baltzer F, Albéric P, Cossa D, Baillif D (2006) Heavy metals distribution in mangrove sediments along the mobile coastline of French Guiana. Mar Chem 98:1–17

Mariotti A, Balesdent J (1990) ^{13}C natural abundance as a tracer of soil organic matter turnover and paleoenvironment dynamics, Geochemistry of the earth's surface and of mineral formation. 2nd International Symposium, Aix-en-Provence, France

Mason RP, Kim EH, Cornwell J (2004) Metal accumulation in Baltimore Harbor; current and past inputs. Appl Geochem 19:1801–1825

Mazuka A, Shunula J (2006) Stable isotope composition of organic carbon and nitrogen of two mangrove stands along the Tanzanian coastal zone. Estuar Coast Shelf Sci 66:447–458

McKee KL, Cahoon DR, Feller IC (2007) Caribbean mangroves adjust to rising sea level through biotic controls on change in soil elevation. Global Ecol Biogeogr 16:545–556

Meehl GA, Washington WM, Collins WD, Arblaster JM, Hu A, Buja LE, Strand WG, Teng H (2005) How much more global warming and sea level rise? Science 307:1769–1772

Meyers PA (1994) Preservation of elemental and isotopic source identification of sedimentary organic matter. Chem Geol 144:289–302

Meyers PA (2003) Application of organic geochemistry to paleolimnological reconstructions: a summary of examples form the Laurentian Great lakes. Org Geochem 34:261–289

Naidu AS et al (2000) Organic carbon isotope ratios (δ^{13}C) of Arctic Amerasian continental shelf sediments. Int J Earth Sci 89:522–532

Nyman JA, Walters RJ, Delaune RD, Patrick WH Jr (2006) Marsh vertical accretion via vegetative growth. Estuar Coast Shelf Sci 69:370–380

Otero XL, Ferreira TO, Vidal-Torrado P, Macias F (2006) Spatial variation in pore water geochemistry in a mangrove system (Pai Matos Island, Cananeia-Brazil). Appl Geochemistry 21:2171–2186

Pikey OH, Cooper JAG (2004) Society and sea level rise. Science 303:1781–1782

Pirazzoli PA (1986) Secular trends of relative sea-level changes indicated by tide gauge records. J Coast Res 1:1–26

Ravichandran M, Baskaran M, Santshi P, Bianchi T (1995) Geochronology of sediments in the Sabine–Neches estuary, Texas U.S.A. Chem Geol 125:291–306

Redfield AC, Ketchum BH, Richards FA (1963) The influence of organisms on the composition of seawater. In: Hill MN (ed) The Sea. Wiley, USA, pp 26–77

Ruttenberg KC, Goni MA (1997) Phosphorus distribution, C:N:P ratios, and (δ^{13}C)oc in arctic, temperate, and tropical coastal sediments: tools for characterizing bulk sedimentary organic matter. Mar Geol 139:123–145

Saito RT, Figueira RCL, Tessier MG, Cunha IIL (2001) ^{210}Pb and ^{137}Cs geochronologies in the Cananeia-Iguape Estuary (São Paulo, Brasil). J Radioanal Nucl Chem 249(1):251–257

Sanders CJ, Santos IR, Silva EV, Patchineelam SM (2006) Mercury flux to estuarine sediments, derived from Pb-210 and Cs-137 geochronologies (Guaratuba Bay, Brazil). Mar Pollut Bull 52(9):1085–1089

Sanders CJ, Smoak JM, Naidu AS, Patchineelam SR (2008) Recent sediment accumulation in a mangrove forest and its relevance to local sea level rise (Ilha Grande, Brazil). J Coast Res 24:533–536

Smoak JM, Patchineelam SR (1999) Sediment mixing and accumulation in a mangrove ecosystem: evidence from ^{210}Pb ^{234}Th and ^{7}Be. Mangroves Salt Marshes 3:17–27

Trask P (1938) Organic content of recent marine sediments. In: Trask D P (ed) Recent marine sediments. Dover Publications, New York, pp 428–453

Twilley RR, Lugo AE, Patterson-Zucca C (1986) Litter production and turnover in basin mangrove forests in southwest Florida. Ecology 67(3):670–683

WCRP (2006) Understanding sea-level rise and variability, summary statement from the World Climate Research Programme Workshop, Paris

Woller M, Smallwood B, Jacobson M, Fogel M (2003) Carbon and nitrogen stable isotopic variation in *Laguncularia racemosa* (L.) (white mangrove) from Florida and Belize: implications for trophic level studies. Hydrobiologia 499:12–23

Woodroffe CD, Thom BG, Chapell J (1985) Development of widespread mangrove swamps in mid-Holocene times in northern Australia. Nature 317:711–712

Zwolsman JJG, Berger GW, Van-Eck GTM (1993) Sediment accumulation rates, historical input, post depositional mobility and retention of major elements and trace metals in salt marsh sediments of the Scheldt estuary, SW Netherlands. Mar Chem 44:73–94